International Journal of Engineering Technology Science and Research
IJETSR
www.ijetsr.com
ISSN 2394 – 3386
Volume 4, Issue 8
August 2017

Paper Skin Platform for Environmental Factor Sensing

Harshad S. Hanmante
Pune Institute of Computer Technology

Prof. A. P. Dhande
Pune Institute of Computer Technology

ABSTRACT

Human skin and hair follicles on it simultaneously help in feeling the surrounding environmentalfactors such as pressure, temperature, humidity, flow and strain.Previously, sophisticated materials and processes have been widely used along with chemically active materials. Although less expensive but shows functional limitations, hence in turn, affecting performance and cost.Here, an easymanufacturingtechnique by using cheap and readily-available household elements likealuminium foil,various daily use papers, tissue papers,office sticky-notepads anda piece of cellulose or synthetic material resembling a true sponge. Sponges to build "paper skin" with real-time sensing capabilities. With this fundamental characteristic of absorption, porosity and dimensions of these materials, sensor network platform which have distributed function is reported,which can sense the basic part of its carrier (Blood pressure, Body temperature,Heart bit rate and Skin hydration) and the nearby environment.Artificial skin can mainly contribute to the robotics domain, bio-medical applications such as in case of burn and acid injury sufferer, and vehicular technology. This technology has the potential to overcome the existing metal and plastic applications in the robotics field due to its inexpensive and flexible nature, easy manufacturing and ready availability of paper material. This technology can further be use in unmanned spacecraft carrying Humanoid in place of Human and this Humanoid will possess all bio, chemical, geological, environmental and many more sensor so that Humanoid will be real copy of Human having all abilities and intelligence.

Keywords

1. INTRODUCTION

Paper describes a unique unanimous extensive material whichtoday is present in every houseas it is cheap due to its low-cost and unavoidably in dailyuse. One of the benefit of using paper substratesfor sensors applications is its permeability and itslarger interfacialarea that supports both high sensitivity and fast response.So far, in many work have used paperas a mass platformor a sensing material for base formation various kinds of devices,spaning from flexible actuatorsfor display and paper-basedMicro-ElectroMechanicalSystem (MEMS)electronics, such as ammonia gas sensors,multi-color LED displays, 3-D antennas,cantilever-type MEMS deflection sensorsand foldablethermochromic displays onpaper. [1–6]Progress in the area ofpaper electronics are in faster dueto its lesser price and eco-friendly benefitsof paper, where themajor attention is to focused towards using elastic cellulosepaper for the fabrication of various typesof sensors, such as humidity, touch, pHvalue analyzer and gas sensors. [7–10] However, theseapproaches still use fragileand costlynanomaterial-basedfunctions, vacuum manufacturingprocesses, and printing techniques, where the paper is still frequent chemically treated andsolution-processed. [11–13]

Flexible artificial skin developments has also fixed their way in the literature,pointing to soft skins for robotic applications by the meansof pressure and temperature sensors integrated on PolyEthyleneTerephthalate (PET) or polyimide (PI) substrates. [14–19] However,the current approaches are still far from being developed as abusinessdue to their fairly expensive manufacturing processes and difficult combination. Improvements in artificial skin integration have shown possibilitiesfor strain, humidity, pressure, and temperature sensing. [20–31]

International Journal of Engineering Technology Science and Research
IJETSR
www.ijetsr.com
ISSN 2394 – 3386
Volume 4, Issue 8
August 2017

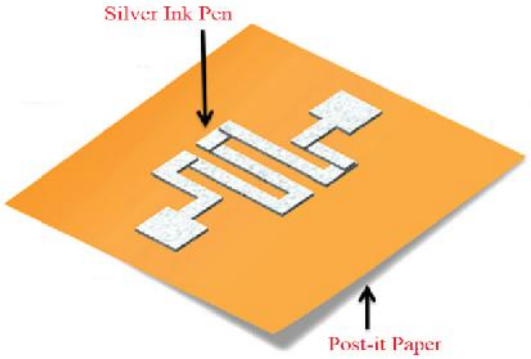

Fig 1(a): Prototype of temperature sensors using silver ink pen and aluminium foil

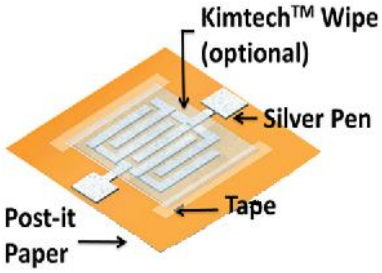

Fig 1(b): Humidity sensor using capacitive designusing post-it paper as sensing material

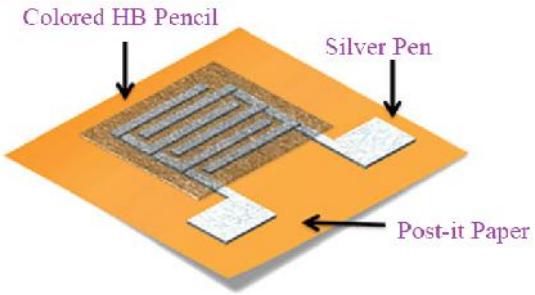

Fig 1(c):A capacitive-based disposable pH sensor

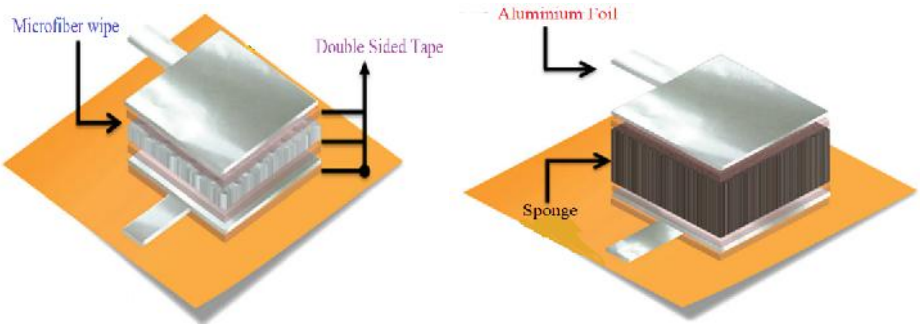

Fig 1(d): "Design 1" pressure sensors using a parallel-plate structure and two different sensing materials: microfiber wipe and a sponge

International Journal of Engineering Technology Science and Research
IJETSR
www.ijetsr.com
ISSN 2394 – 3386
Volume 4, Issue 8
August 2017

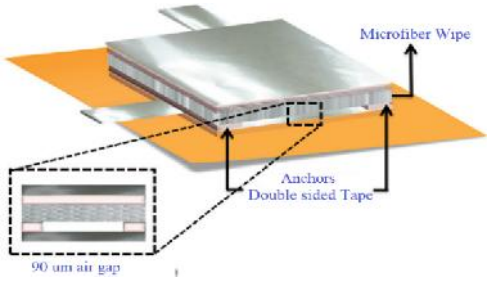

Fig 1(e):Structure of "Design 2" of pressure sensor based on air-gap structure.

2. DESIGN AND OPERATION

To design sensor, a3M Post-it Note is used as a flexible paper substrate,aluminium foil and silver ink pen are use for the contact pads and interconnects. A spectrum of materials and structures are used for the sensing film to achieve the preferred performance and application. Table S1 shows materiallist used for each specific sensor, highlighting their important characteristics. Both temperature and pH sensors have a resistive functionality, whereas both humidity and pressure sensors rely on a capacitive-based sensing. Detailed design and process flow of the sensors are explained in Figure1& discussed in the Experimental Section. In the following sections, details of every sensor's principle of operation and choice of material as shown inlist l.

2.1 TEMPRETURE SENSORS

Temperature sensor is either cut out of aluminium foil or drawn with the silver conductive pen on the Post-it paper.

(Fig.1a).The aluminium foil has an electrical resistivity of 3.83×10^{8}Ohm, whereas the silver pen on paper has a resistivity in the interval of 0.05–0.2 Ω^{-1}. This slight variation in the electrical conductivity is due to the variations in filling density. The resistance of the sensor will vary in accordance with temperature due to phonon vibrations in the lattice structure of the metal, that will increase the spacing between atoms and reduce the ability of the material for properly electrical current conduction, causing an increase in resistance. The relative resistance change versus temperature f(T) = $\Delta R/R$ of temperature resistors is commonly represented by temperature coefficient values of the of resistance (TCR). The TCR is defined as the slope of the $\Delta R/R$ = f (T) curve and can be expressed by

$$TCR = \frac{\left[\frac{\Delta R}{\Delta T}\right]}{R} \qquad (1)$$

Where TCR [in°C^{-1}],ΔR [in Ω] is the change in resistance corresponding to ΔT [in°C] the change in temperature and R [in Ω] is the initial resistance of the sensor. The theoretical TCR of silver and aluminium at 20 °C are, respectively, 0.0038 and 0.0039 °C −1.

2.2 HUMIDITY SENSOR

For the capacitive humidity sensors (Fig.1 b),paper withholdingan advantageous property for measuring humidity due to its porous cellulose-fibernature,the adsorption and desorption of moisture on paper relative to humidity levels area well-known phenomenon.Since paper is hygroscopic,as humidity level increases,more water molecules adsorb to the hydroxyl groups on the surface of the paper, changing the relative permittivity and altering in turn the capacitance of the sensor. Water has a relative permittivity of $\varepsilon_{r,water}$= 80.1 at 20 °C, thus the permittivity of paper is expected to increase, leading to an increase in capacitance as humidity levels rise (Equation(2)

$$C = £_0£_r A/d \qquad (2)$$

where C is the capacitance of the sensor [in F], $\varepsilon_0$is the vacuum permittivity ($\varepsilon_0 \approx 8.854 \times 10^{-12}$[$Fm^{-1}$]), $\varepsilon_r$is the

International Journal of Engineering Technology Science and Research
IJETSR
www.ijetsr.com
ISSN 2394 – 3386
Volume 4, Issue 8
August 2017

relative permittivity of the dielectric material in between the two conductive fingers, and *d* is the separation between the parallel conductive plates (in m).As an optional step for stability in measurement fluctuations, sensor structure is covered with a sheet of KIMTECH wipe, which shows to reduce electrical discharges and has a relative permittivity very close to that of air (Table S1).

2.3 pH SENSOR

For the pH sensor, pencil of grade HB acts as the sensing film (Figure 1 c). It has 68% carbon,26% clay and the electrical resistivity is calculated to be $\rho = 1.85 \times 10^{-4}$ Ω m. Note thatρ is highly dependent on the content of carbon and decreases as the percentage of carbon increases. The principle of operation relies on measuring the change in resistance upon exposure to different pH levels. Since paper substrate is sensitive to moisture, once exposed to a solution (regardless of the pHlevel), moisture level in the paper will increase and saturate increasing the electrical conductivity of the paper and inducing a change in the resistance of the sensor. In fact, resistance of paper was found to decrease with water molecules adsorbed on its surface. Pure water should be an excellent insulator; however, water undergoes autoionization in the liquid state when two water molecules form one hydroxide anion (OH^-) and one hydronium cation (H_3O^+). And since water is a great solvent, it often has some tiny impurities dissolved in it (e.g., salt), which can conduct electricity. To prove this statement, the resistance of our pH structure testedwithout the graphite film on topand measure resistance before and after putting it in contact with water. With no water, the resistance is measured to be R_{paper} = 258 MΩ, and with added water the resistance decreases to $R_{paper+water}$ = 1.07 MΩ. This translates into a total decrease in the structure resistancebe negligible compared to the high conductivity introduced by the pencil layer and constant for all solutions under study. In this case, the dominant effect is the redox reaction occurring between the graphite and hydroxyl ions in the corresponding aqueous solutions. An acidic solution has higher concentration of hydrogen ions H + than water, and a basic solution has higher concentration of hydroxide ions OH^-. The sensing mechanism can be explained by the adsorbed ions (hydroxonium ions H_3O^+ and hydroxyl ions OH^-). When exposed to an alkaline solution, the carbonyl functional group goes through areduction step (gaining electrons e^-), eventually transforminginto methane (CH_4) the most highly reduced state, decreasingthe resistance with respect to neutral solution resistance. Conversely, when exposed to an acidic solution, the carbonbased film goes through an oxidation step (loses e^-), eventually becoming CO_2, which is the most highly oxidized state, increasing the measured sensor's resistance.

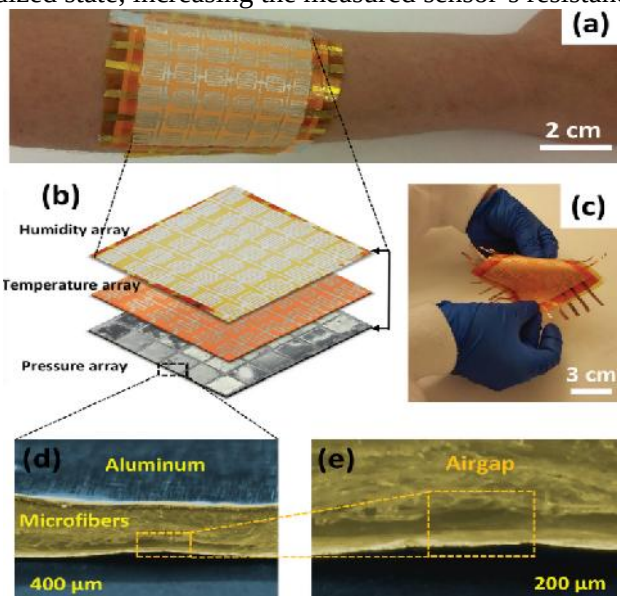

Fig 2: a) Digital photograph of flexible 6 × 6 "paper skin" wrapped around an arm b) Schematic of 3D stacked paper skin structure composed of pressure, temperature, and humidity arrays. c) Digital photograph of flexible temperature sensors array. d) High-resolution photograph of the cross-section of the pressure sensor "design 2," showing the microfiber wipe sandwiched in aluminium foil with an air-gap cavity. e) Zoom in picture of the air-gap assembly.

2.4 MULTIFUNCTIONAL FORCE SENSOR

Principle of operation of pressure sensors (Fig.1d) isdescribed in Equation (2). As applied pressure increases, the dielectric thickness decreases, increasing the output capacitanceof the sensor.In fact, due to the elastic deformation and porous properties,the sponge will vary in thickness as it is exposed to various external forces. Similarly, the cleanroom wipes are composed of multilayer microfiber construction; this texture allows for high sensitivity and deformation under mechanical stimuli.In order to further improve the sensor's response to lower pressure regimes, an air-gap-based design was implemented (Fig.1e). This geometry allows detection of lower pressure due to the ultrahigh compressibility of air.Infact, it has been shown that electrical signals from vibrations are dramatically amplified when an air gap of few micrometers in size is implemented in the sensor's structure.

2.5 PAPER SKIN INTEGRATION

Finally, 6 × 6 artificial paper skin through the superposition of three layers of sensor networks is constructed as shown inFigure 2. Details about the array design are described in the Experimental Section. The pressure-sensing platform providesmultifunctionality for force, touch, motion, direction, and proximity sensing due to its unique structure illustrated in the cross-sectional photograph in Fig.2d, with a focus onto its air gap shown in Figure 2 e. This stacking configuration allows for simultaneous localized sensing of various external stimuli per pixel, bringing together extensive sensing functionalities in a low-cost and sustainable manner.

3. MATERIALS CHARACTERIZATION AND DISCUSSION

Thickness, electrical resistivity, and relative permittivity are the essential material properties required to build our devices and understand their behaviour. These characteristics are summarized in Table S1 (Supporting Information). Thickness was obtained through a high-accuracy digital micrometer electrical resistivity using a four-point probe resistivity measurement, and relative permittivity was calculated from the measured capacitance of a 3 × 1 cm^2 capacitor, using the studied material as the dielectric.

3.1 TOPOGRAPHY AND POROSITY OF HOUSEHOLD MATERIAL

To study the surface topography and porosity of the different materials,SEM(Scanning electron microscopy) wascarried out. For sample making of the post-it note, To remove dust particles,the piece of paper was blow-dried with nitrogen (N_2) and then coated with 2 nm layer of Iridium (Ir) to prevent charging during imaging. The SEM imagein Fig.3a reflects the fiber structure of the post-it paper through the apparent mesh of cellulose microfibrils. Cellulose is hydrophilic and insoluble in water, which makes it perfect for our humidity sensing purposes. As for the sponge and the microfiber cleanroom wipe, the samples were sputtered with a 2 nm layer of Ir to prevent charging. SEM images in Figure 3b,c confirm the porous nature of our chosen materials. This porosity allows more compressibility and deformation; an advantageous property for improved low-pressure sensitivity. It is identified that the sponge shows a different structure than the cleanroom wipe, where it displays a network of hallow hexagonal microstructures (pores), whereas the polypropylene (PP) e illustrates a network of randomly oriented microfibril threads. As shown in Figure 3 c, the wipe reveals low density of microfibrils, translating into higher sensitivity to small loads. In fact, the synthetic sponge is made out of foamed polyester (PES), which is rugged, stiffer and has higher density than the PP found in the cleanroom wipes (DPP=0.91 g $cc^{-1}$$D$PES = 1.38 g cc^{-1}). Besides, elongation is much higher for PP, which gives better elasticity and thus more compressibility.Therefore, it is expected that the cleanroom wipe-based sensor will demonstrate a higher sensitivity to pressure, whereas the sponge-based sensor will show a wider range of operation in the high pressure regime, due to its larger thickness.

International Journal of Engineering Technology Science and Research
IJETSR
www.ijetsr.com
ISSN 2394 – 3386
Volume 4, Issue 8
August 2017

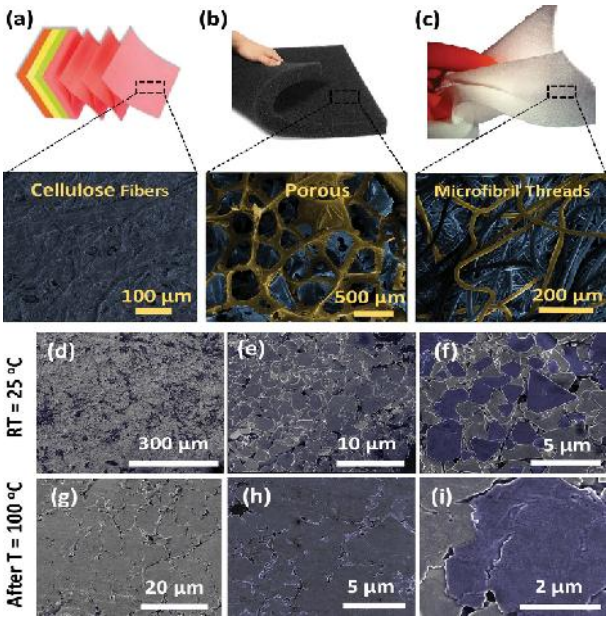

Fig 3: Optical and scanning electron microscopy (SEM) images highlighting the different porosity structures and topographies of a) Post-it paper, b) sponge, c) and cleanroom microfibril wipe. All materials were coated with 2 nm of Iridium (Ir). d–f) SEM images of silver (Ag) ink on post-it paper drawn at room temperature. g–i) SEM images of the same silver ink sheet after heating at 100 °C and left to cool down at room temperature.

3.2 INTERCONNECTS STABILITY

Since silver ink was used for designing temperature sensors and integration networks, stability of thesilver ink interconnects at high temperatures is studied. SEM of a silver ink sheet on top of the post-it paper is performed before and after heating the sample to 100 °C. Resistance values were extracted for both cases only after the temperature of the surface came back to room temperature (T = 25 °C). Figure 3 d,f shows the SEM images of the silver (Ag) ink particles before heating, where we can clearly distinguish the fairly uniform distribution of Ag hexagonal microstructures. After heating to 100 °C, room temperature images in Figure 3 g,i indicate that the silver-based gel-ink pen has expanded and the enlarged Ag microstructures have superimposed. The diffusion temperature of pure Ag is determined to be above 630 °C.However the circuit scribe conductive pen composition is like that of any commercial gel-ink pen, except the color pigments in the pen have been replaced by silver particles. This being said, a gel medium exhibits a high liquid viscosity, described by the dynamic viscosity (μ),wherethe viscosity of the medium tends to decrease as temperature increases, translating into a liquefied medium that promotes the superposition of Ag particles. The dynamic viscosity (μ) is exponentially dependent on temperature by Reynolds' model by Equation (3)

where$T$ is temperature [in °C], μ is the viscosity of the liquid [in Pa s] and μ 0 and b are empirical coefficients of the model. Moreover, at elevated temperatures, the silver particles have undergone thermal expansion in which their volume expands in response to temperature through heat transfer. The volumetric thermal expansion coefficient α v of any medium is described by Equation (4)

where,$V$is the medium's volume [m^3],T is the temperature [K], and p indicates that the pressure is held constant during expansion. The linear thermal expansion coefficient of silver is α Ag = 18 × $10^{-6}K^{-1}$and since silver is an isotropic material, then the area thermal expansion coefficient becomes 2 α Ag and the volumetric expansion coefficient is 3 α Ag . The results display an irreversible process where the sheet resistance of silver ink interconnects decreases due to an improvement in fi lm density. Fig. S1 illustrates the decrease in resistance after the silver ink is heated to temperatures up to 100 °C. Resistance decreases from 4.75 Ω at

International Journal of Engineering Technology Science and Research
IJETSR
www.ijetsr.com
ISSN 2394 – 3386
Volume 4, Issue 8
August 2017

room temperature (25 °C) down to 2.83 Ω after heating to ≈95 °C, given that the resistance value was taken after the conductive ink cooled down to room temperature.

4. PERFORMANCE ANALYSIS AND DISCUSSION

4.1 SENSITIVITY AND REAL-TIME STUDY OF TEMPRETURE DETWCTION

First, the temperature sensor behaviour, comparing the silver-ink-based sensor with the aluminium-foil-based sensorwasevaluate. In this case, the silver-ink-based sensor was used after it was heated to 100 ^{0}C and cooled down to insure material stability.Then, characterization of each sensor on a thermal chuck probe station was done, where the chuck was heated from 25 ^{0}C up to 100 ^{0}C with steps of 10 ^{0}C. For precision, the temperature on the surface of the sensor is measured using a thermocouple and the resistancevalue is collected using a digital multimeter. Figure S2(Supporting Information) shows that both sensors exhibit a linearbehaviour where resistance increases with respect to temperature. Theestimated TCR for aluminium foil and silver ink pen are found to be$TCR_{exp,Al}$ = 0.00383 $^0C^{-1}$and $TCR_{exp,ag}$=0.00372 $^0C^{-1}$respectively. In an experiment values very closely match the materials' theoretical TCR values of $TCR_{th,Al}$= 0.0039 $^0C^{-1}$with a relative % error of 1.8% and $TCR_{th,Ag}$ = 0.0038 $^0C^{-1}$with a relative % error of 2.1%. It is shown that the silver-inkbasedsensor is nine times more sensitive than the aluminium foil-based temperature sensor, with respective sensitivities ofS_{Ag}= 0.0107 $^0C^{-1}$ and S_{Al}= 0.00115 $^0C^{-1}$.For arraying purposes, we continue our studies with thesilver-ink-based sensor. temporal study measurements was carried out, The sensor to very commonexternal stimuli was exposed.test the temperature sensor's test is carried out then for real-time response to human touch(T = 37 ^{0}C) (Figure 4a,b), human exhaled breath (around 42 ^{0}C)(Figure 4 c,d), and from a lighter flame positioned 10 cm awayfrom the sensor ($T \approx 85^0$C) (Figure 4(e)). Figure S3(a) (Supporting Information) that shows the Gaussian/Lorentz an profile of the sensor's response to human touch. The maximum change in voltage is ΔV = 1.38 mV corresponding to a change in temperatureof ΔT = 12 ^{0}C relative to room temperature. The total response time of the sensor is 7.37 s and the total time for the sensor to recover its initial state is 10.32 s. The recovery takes the shape of an exponential decay from which we can retrievethe rate of decay by extracting the mean lifetime □□or halflife$t$ 1/2 of the sensor, corresponding to the time required forthe sensor to fall back to half of its initial value. In this case,the half-life of the sensor was determined to be t1/2 1.88 s. Forbreath temperature detection (Figure S3b, Supporting Information),the maximum change in voltage is 0V *to* 2.34 mV corresponding to a change in temperature of ΔT = 20 ^{0}C relative toroom temperature. The sensor exhibits a spike response timeof 421 ms, with a total recovery time of 7.16 s. For the finaltest, we position the flame of a lighter about 10 cm away from the surface of the sensor. Figure S3c shows the originated change in voltage in response to theflame's heat. The peak change recorded is ΔV = 6.59 mV corresponding toΔT = 60 ^{0}C. The total response time is about 1.89 s,with the fastest total recovery time of 5.27 s.This proposed paper-based temperature sensors show high sensitivity tothe point of detecting the spectroscopic behaviour of the exhaled breath (Figure 4 d). This signal originates from the pulsating nature of our breathing process, controlled by our heart rate.an ultrafast response and recovery times of 421 ms and5.27 s, respectivelyWas reported , compared to 20 s response and 30 s recovery time reported in the previously published literature.

4.2 MOISTURE RECOGNITION AND TIME STUDY OF HUMIDITY SENSING

Aresponse of humidity sensor was considered by exposing it tothree different values of known humidity levels: room temperature(46%), human breath (76%), and water vapour (97%). Thesehumidity values were determined using a commercial humiditysensor. As expected, Figure S6a shows a nearly linear increase in the capacitance as humiditylevels increase. The maximum calculated sensitivity is 0.18%/%RH, which is quite low compared to values reported in the literature, but still we show a very repeatable behaviour withfast adsorption and desorption times.Humidity in the surrounding environment was led in realtimefor different external stimuli shown in Figure 4 g–j. Theexperimental setups are clarified in the Experimental Section, andshown in Figure 4 g,h for the water vapour test. For humid breathtesting, Figure 4 i shows an increase of 0.025 pF in capacitanceas a response to 76% relative humidity. Figure S4b shows a very fast total response time of 2 s, withan exceptional growth behaviour with half-life time t ½ = 0.34 s.As for the recovery of the sensor, desorption follows a Boltzmann profile, with total recovery time of 1.33 s. For damp weather

International Journal of Engineering Technology Science and Research
IJETSR
www.ijetsr.com
ISSN 2394 – 3386
Volume 4, Issue 8
August 2017

detection, we use a water vapour setup, where the time study inFigure 4 i demonstrates that the activation of the wind tunnel fanhas no effect on the response of our sensor, guaranteeing that thebehaviour seen is solely from the vapour humidity. In this case, thesensor has a total response time of 1.2 s and a recovery time of3.2 s (Figure S4c, Supporting Information). Typically, although the sensitivity reported is not so high, however we report veryfast response and recovery times of ≈1 s and 1.33 s, respectively,nearly ten times faster than the ones found in the literature usingcomplex fabrication processes and expensive materials. The observed faster response and recovery times are respectivelyattributed to faster absorption and evaporation ratesin porous surfaces (e.g., cellulose paper in this work) in contrastto the flat nonporous materials commonly used in theliterature. The faster absorption in porous media is driven bythe capillary pressure, which is inversely proportional to thepore size, but also the permeability of porous materials scaleswith the square of the pore size. Thus, this dynamic superimpositionof both mechanisms for liquid absorption leadsto an overall faster absorption time in heterogeneous porousstructures. In this case, the absorption time can be expressedeither by the classic Washburn's Law for simple porous constructs(Equation (5)), or by Darcy's law (Equation (6)) for a more accurate representation of the absorption process ofwater in a heterogeneous porous medium:

5. ARTIFICIAL SKIN EVOLUTION COMPARISON

Direct comparison between this work and several of the artificial skin platforms being developed by pioneers in the

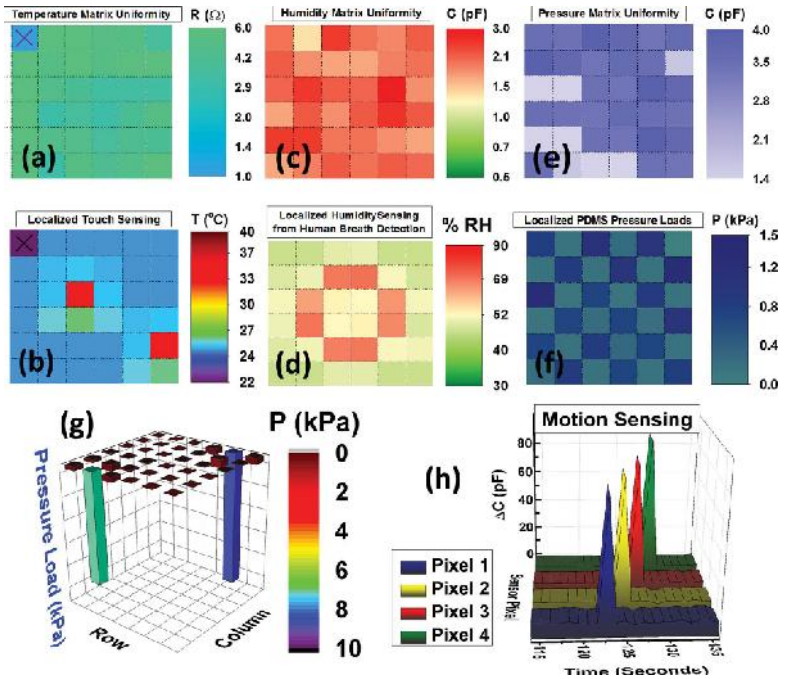

Fig 6(a): Temperature array pixel distribution. Pixel R1-C1 is damaged. b) Spatial mapping of temperature with stimulus exerted on pixels R3-C3 and R5-C6. c) Humidity array pixel-to-pixel uniformity. d) Spatial mapping of humidity in response to stimulus simultaneously applied on pixels R2-C3, R2-C4, R3-C2, R3-C5, R4-C2, R4-C5, R5-C3, and R5-C4. e) Pressure array pixel uniformity. f) Spatial mapping of pressure in a "Chess-board" pattern. g) 3D bars representation corresponding to localized 8 kPa loads on pixels R1-C2 and R6-C5. h) Simultaneous temporal and spatial mapping of motion sensing from four different pixels.

International Journal of Engineering Technology Science and Research
IJETSR
www.ijetsr.com
ISSN 2394 – 3386
Volume 4, Issue 8
August 2017

Field shows that our paper skin maintainsthe desirable high performance of sensors, while displayingmore valuable features through the integration of variousfunctionalities with the most affordable materials possible.Table 1 indicates a summary of the main characteristicsfound for E-skin platforms based on sensing material used,sensitivity, response time, recovery time, working range, andmost importantly cost. Paper skin shows to be clearly themost inexpensive and advantageous option preserving therequired high performance of sensors platform.

Table 1. Summary of E-skin sensors characteristics. Table comparing this work to several artificial skin platforms, displaying differentiation between performance, material, functionality, and cost.

References	Functionality	Sensing Material	Sensitivity	Response Time	Recovery Time	Working Time	Cost
Biological Skin	Force	N.A.	0.0.18 – 0.078 [kPa-1]	30-50 ms	< 2kPa	N.A.	_
Takei	Temperature	CNT-P.EDOT: PSS on PET	0.0025 [0C]	1s	19s	N.A.	↑
	Strain / Pressure	AgNP-CNT on PE	0.13 [mN]	2.5s	22s	N.A.	↑
Bao	Pressure	PDMS	0.025 – 0.2 [kPa-1]	2.5s	300ms	0 – 35 [kPa]	←
	Temperature	P (VDF-TrFE) & Ba TiO3 NPs	N.A.	2.5s	N.A.	N.A.	↑
Javey	Pressure	CNTs;NWs	0.09kPa-1; 0.033kPa-1	2.5s	< .01s	<6 kPa; 2–15 [kPa]	↑
Fang	Humidity	RF-aerogels	0.56% / %RH	2.5s	N.A.	N.A.	↑
D-H Kim	Pressure/ Strain	Si nanoribbons	0.0041 [kPa-1]	2.5s	N.A.	N.A.	↑
Han	Humidity	COOH functionalised SWCNTs on cellulose paper	0.06% / %RH	2.5s	120s	N.A.	↑
This Work	Temperature	Silver ink pen	0.00372 [0C]	2.5s	5.3s	N.A.	←
		Aluminium foil	0.00383 [0C]	N.A.	N.A.	N.A.	↓
	Humidity	Post-it paper	0.18% / %RH	1.2s	1.33s	Full range of RH	↓
	Force (Pressure, flow sensing)	Cleanroom napkin / sponge	0.16 [kPa-1]	< 130 ms	< 130 ms	> 0.009 [kPa]	↓
	Proxmity	Aluminium foil	N.A.	N.A.	N.A.	13cm	↓

CONCLUSION

Using only off-the shelf resources, we demonstrated the firstever recyclable paper-based skin capable of detecting temperature,humidity, pH, pressure, touch, flow, motion, and proximityat a record-breaking distance of 13 cm. The fabricatedsensors show reliable and consistent results, and the pressurearraydisplayed exceptional capability in differentiating multipleexternal stimuli. The simplistic fabrication process and lowcostmaterials used in this work make this flexible platformthe lowest cost and accessible to anyone,

without affecting performancein terms of response and sensitivity. Additionally,the proximity and motion features obtained in this work illustratethe possibility for paper-based touchless motion systems,bringing the user-to-computer interface experience to a wholenew level. Paper skin is an affordable all-in-one flexible sensingplatform, applicable for emerging applications, such as healthmonitoring, 3D touchscreens, and human–machine interfaces,where sensing diversity, surface adaptability, and large-areamapping are all essential. Future works include analysis of performancecharacteristics and reliability of the fabricated skinunder various mechanical deformations (flexing, stretching,etc.). Although further sophistication is possible, at the presentstage the demonstrated “paper skin” integrates the maximumsensory functions of a human skin in a cost effective andeco-friendly manner. Familiar